SMALL SCALE SOLAR ORC SYSTEM FOR DISTRIBUTED POWER

Matthew S. Orosz,[1] Amy Mueller[1] Sylvain Quolin,[2] and Harold Hemond[3]

[1] Doctoral Candidate, Massachusetts Institute of Technology, Civil and Environmental Engineering; Solar Turbine Group, 15 Vassar St. 48-216 Cambridge MA USA, (508) 245-6199, mso@mit.edu

[2] Doctoral Candidate, ME, University of Liege [3] Professor, CEE, Massachusetts Institute of Technology

Abstract

A solar thermal organic Rankine cycle (ORC) can provide affordable energy supplies in remote regions. The advent of low-cost medium temperature parabolic trough collectors and ORC technology taking advantage of mass produced fluid machinery from HVAC industries are enabling developments for the production of small scale autonomous power generation units. Construction and testing of this type of system is discussed, including benchmarking of scrolls expanders (up to 75% isentropic effieiency) and the field testing of solar collectors (50% thermal efficiency at 150°C operating temperatures) with a nominal cost of \$80 m^{-2}. These results have led to the construction of a full-scale 3kW solar ORC power system designed to support a rural health clinic in Lesotho in southern Africa.

Keywords: Solar Thermal, Organic Rankine Cycle, ORC, Distributed Power Generation

1. Introduction

Recent analysis suggests that small (i.e. kilowatt) scale Concentrating Solar Power (CSP) systems with organic Rankine cycle (ORC) power blocks may compete with photovoltaics (PV) and diesel generators on a levelized cost of electricity (LCOE) basis for off-grid duty [1]. Keys to successful and economically viable deployment of this technology lie in i) optimizing the parabolic trough solar collectors for medium temperature thermal output (<200°C), ii) use of an ORC embodying cost-effective expander-generator components (i.e. modifications of off-the-shelf equipment) [2] and iii) use of autonomous to match system operation to fluctuating thermal input from the collector array. This paper discusses the design and testing of components for a 3kW Solar ORC both on test benches (MIT, U. Liege) and in the field (Lesotho, Africa).

2. Small Solar ORC Concept

For decades solar ORC concepts for community power supplies have been extensively discussed but rarely implemented [3-5]. Often the availability of lower-cost electricity from a power grid is cited as an impediment to adoption of solar ORC or other renewable sources of electric power [3]. Rural regions of many countries lack centralized grid infrastructure, however, and in these circumstances distributed small scale CSP achieving economies of scope (many modular units with mass produced components) may be economically competitive with alternative off-grid power technologies, i.e. photovoltaic (PV) panels and diesel generators, which have a levelized cost of electricity (LCOE) in the \$0.30-\$0.50 kWh^{-1} range [6-8]. Modern CSP technology that achieves \$0.15-20 kWh^{-1} electricity exists in large-scale installations [9], suggesting that if it could be successfully scaled down, is could be cost effective for use in applications typically served by PV or diesel generators (e.g. clinics, schools, small enterprises). Several practical challenges must be addressed to meet this objective, including (1) the high initial and maintenance costs of solar collector receiver elements and mirror facets, (2) the unavailability of small thermal power blocks, and (3) the need for unattended operation. We propose a small-scale solar thermal ORC design that addresses these challenges by making use of simple, proven parabolic trough technology and a novel power block comprised of off-the shelf components and materials. These components include scroll compressors, heat exchangers, pumps and working fluids sourced from the HVAC and automotive industries; industrial motors and reflective aluminum sheeting; standard steel structural and pipe sections; and standard microcontroller and power electronics (**Table 1**). An additional design challenge arises from the choice of a thermal power plant: namely the requirement for a cooling reservoir. Because the availability of water sources varies

depending on site-specific conditions, and given the water constraints faced by many regions where distributed power generation is most appropriate, air-cooling is adopted here as a more general approach. We describe below the technical outline of the proposed system and present information on bench and field testing through a collaboration between MIT, University of Liege, STG International and the Government of Lesotho's Appropriate Technology Services. A functional diagram of the system is shown in (**Fig. 1**).

Table 1: Components for a small scale Solar ORC (numbers refer to Fig. 1).

Component	Description	Industry Supplier	Notes	Approximate Cost Data *
1. Glazing	Duran 50	Schott Solar	Borosilicate 1.25m L 80mm OD 5mm Thickness	65 USD/pc
2. Reflector	Miro-4	Alanod	1.25m W 0.4mm Thickness 95% Reflectivity	15 USD/kg
3. Working Fluid	HFC-245fa	Honeywell Solvay	b.p. 15.3C c.p. 153C GWF 950, ODP zero - non flammable	33 USD/kg
4. WF Pump	Plunger	Hypro, Various	Common pressure washer pump	300 USD/pc
5. Heat Trasfer Fluid	Mono Ethylene Glycol	Various	b.p. 186C; used as antifreeze	3.50 USD/Liter
6. HTF Pump	V-20 Power Steering	Vickers	Long haul truck power steering pump	290 USD/pc
7. Fluid/tracking motors	24VDC	Leeson, Various	High efficiency permanent magnet drive	300 USD/pc
8. Expander-generator	Hermetic Scroll-Induction machine	Copeland	Commercial HVAC compressor	1000 USD/pc
9. Heat Exchangers	Brazed Plate BP-410-30	ITT Brazepak, Various	Compact high efficiency heat exchanger	500 USD/pc 40 USD/kW
10. Air Condenser	Forced convection finned copper tube	Carrier, Various	Standard HVAC coils 3 rows 3/8ths tubing	45 USD/kW rejection
11. Sensor based Control systems	Microcontroller and feedback loops	MIT/STG	Solar ORC system optimization	1200 USD

* Note: Costs and specifications are based on data gathered 2006-2009, are subject to change, and generally do not represent official claims of the manufacturer

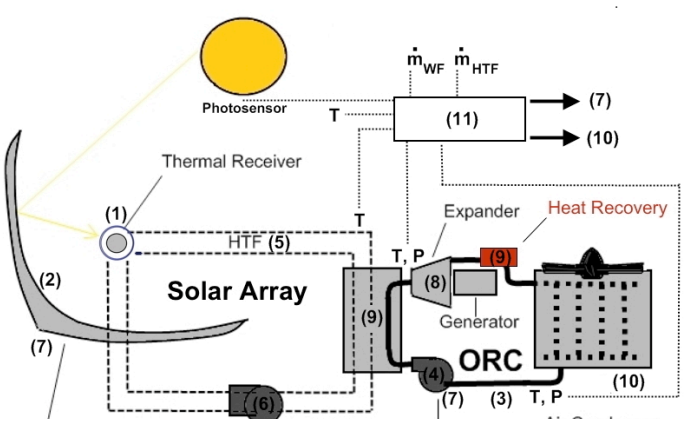

Figure 1: Schematic overview of the Solar ORC (numbers refer to Table 1).

3. Medium Temperature Low Cost Parabolic Troughs

Solar thermal power plants face tradeoffs between cost and thermal efficiency, particularly in light of countervailing trends in thermal efficiency between collector elements and heat engines. While the thermodynamic efficiency of heat engines increases with operating temperature, solar absorbers will have greater thermal losses due to convection and radiation [10]. Mitigating these losses under high-temperature operation, e.g. by means of selective high absorbtivity and low emissivity coatings and evacuated glass glazing, entails higher costs in materials and manufacturing. These features may be economically justified in megawatt-scale installations, where large collector production volumes lead to lower specific costs and where the cost of land lease is an important consideration. Where the cost of space is not a constraint, however, and where small capacity units of deployment are preferred, optimization for the lowest LCOE may lead to medium temperature designs involving lower thermal efficiencies and increased footprint, e.g. from ~ 20 m^2/kWe in a typical large scale CSP plant [11] to ~ 35m^2/kWe in a medium temperature CSP plant. Exemplary data are shown in **Table 2**. Each collector type will exhibit a different optimal system operating temperature (**Fig. 2**) when coupled with a well-designed practical heat engine (i.e. one that approaches a Curzon-Ahlborn efficiency of ~ $1-\sqrt{(T_C/T_H)}$ [12]).

Table 2: Comparison between high and medium temperature Solar Rankine Cycles.

	Collector Cost	Power Block Cost [Type]	Solar to electric efficiency	Array Area [i] m^2/kWe	$/W [ii]
High Temperature 350°C	$220 /$m^2$	$1.5/W [Steam Rankine]	13%	20	3.5
Medium Temperature 150°C	$80 /$m^2$	$2/W [ORC]	7%	35	3.3

Source: High Temperature Systems [7], Medium Temperature (this study)
i Total footprint includes space between collector rows
ii Excludes installation, O&M, and financing

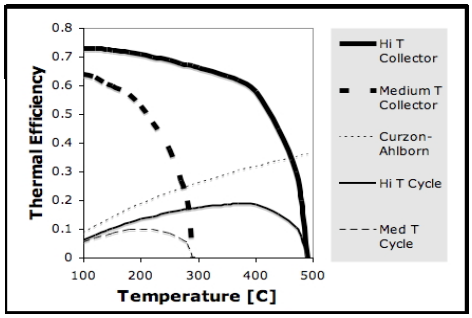

Figure 2: Efficiency vs. Temperature curves for semi-idealized high and medium temperature systems.

Table 3: Parameters used for collector performance prediction, based on a collector model modified from Forristall (2003).

Parameter	Value	units	Description
M_dot MEG	0.4	kg s^{-1}	HTF mass flowrate
T inlet	119	°C	Inlet temperature
T outlet	150	°C	Outlet temperature
W Aperture	2.5	m	Collector tip to tip width
D2	0.057	m	Absorber pipe ID
D3	0.062	m	Absorber pipe OD
D4	0.07	m	Glazing ID
D5	0.08	m	Glazing OD
L	30	m	Total absorber length
I	830	W m^{-2}	Solar direct radiation
V wind	6	mph	Windspeed
T ambient	14	°C	Ambient temperature
Absorber ε	39	%	Solec Solkote emissivity
Absorber α	91	%	Solec Solkote absorptivity
Annulus gas	Air		
Glazing τ	93	%	Glazing transmissivity
Reflectivity	94	%	Mirror reflectance
Thermal η	57	%	Overall collector efficiency
Thermal Power	35.3	kW	Absorbed power

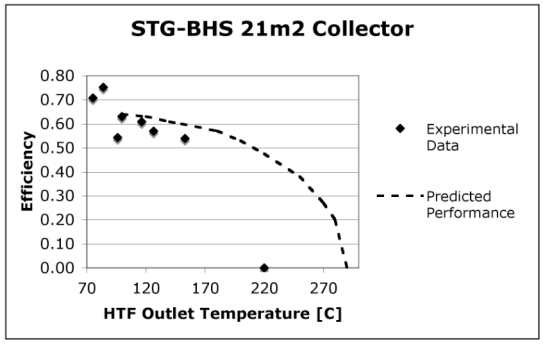

Figure 4: Measured and predicted (EES trough model) performance of the STG type medium temperature collector.

Figure 3: 1 kW Solar ORC (2-axis tracking version) in field trials in Lesotho (STG 2007).

For our proposed sysetm we have designed and tested a low cost parabolic trough module that can be deployed in either 2-axis or single axis tracking configuration (**Fig. 3**). The trough collectors use Miro-4 reflective sheeting (supplied by Alanod Corporation) and feature a glazed glass air-filled annulus receiver operating at 150°C. Monoethylene glycol is used as the heat transfer fluid (HTF). At a 150°C outlet temperature, a 57% thermal efficiency is predicted by a modified version of Forristall's 2003 parabolic trough collector model in Engineering Equation Solver (EES), using parameters adjusted for operating conditions in southern Africa. Simulation results are shown in **Table 3**. Field testing of the STG-01 (21 m^2) and STG-02 (24 m^2) collectors in Lesotho in 2007 revealed good agreement with model prediction at operating temperatures up to 150°C, as shown in **Fig. 4**, with variation attributed to different collector geometry (15m absorber length vs. 30m used in model), unrecorded variations in windspeed and ambient temperature, variable insolation levels (800-950 W m^{-2}) and variable HTF flow rates (0.1-0.2 kg s^{-1}). There

is a noticeable gap between observed (220°C) and predicted (290°C) stagnation temperatures, but only modest differences are seen at 150°C. Overall, the collector units demonstrated an acceptable thermal efficiency exceeding 50% at a cost of $80 m^{-2} including local labor.

Another important feature of collectors is the use of readily available materials and adaptability to manufacturing methods suitable to remote worksite construction. The STG collector design uses steel frames welded onsite, with the appropriate geometry derived from a field deployable CNC-machined aluminum jig. The steel frame uses standard steel sections for lateral and longitudinal frame members, as well as round steel geodesic wraps for torsional stiffness (**fig. 5**).

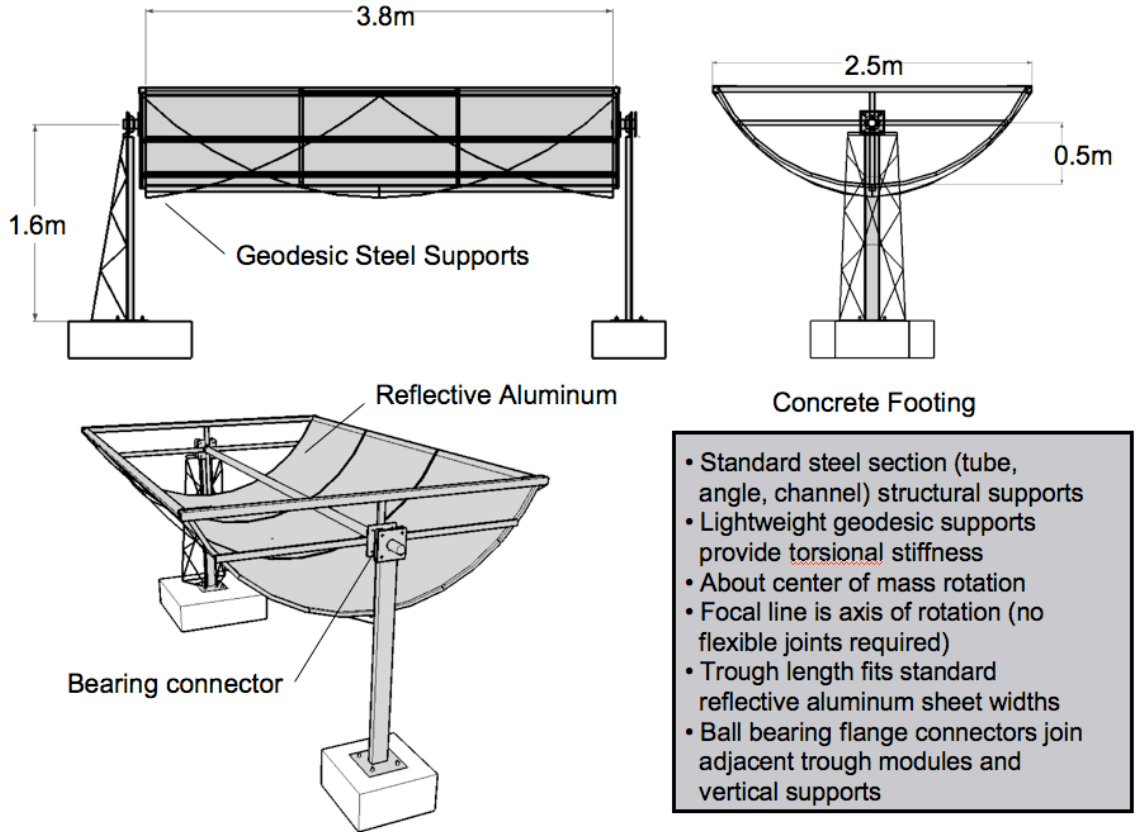

Figure 5: STG-03 Collector (single axis version) currently in testing for powering remote health clinics.

4. Low Cost, Robust ORC

Currently, ORC units suitable for solar power generation are commercially available only in capacities above a few hundred kilowatts (e.g. Ormat, UTC etc). For the application considered here, an easily manufactured, cost-effective ORC unit is required in the range of one to tens of kilowatts. We have proposed to adapt commercially available compressor machinery to this purposes. Given the many interlocking parameters to be optimized in ORC design, including but not limited to choice of working fluid, lubricant, pressure ratio etc., it appears necessary both to characterize candidate machines through thermodynamic modeling efforts, as well as to experimentally determine their isentropic efficiency and dynamic characteristics.

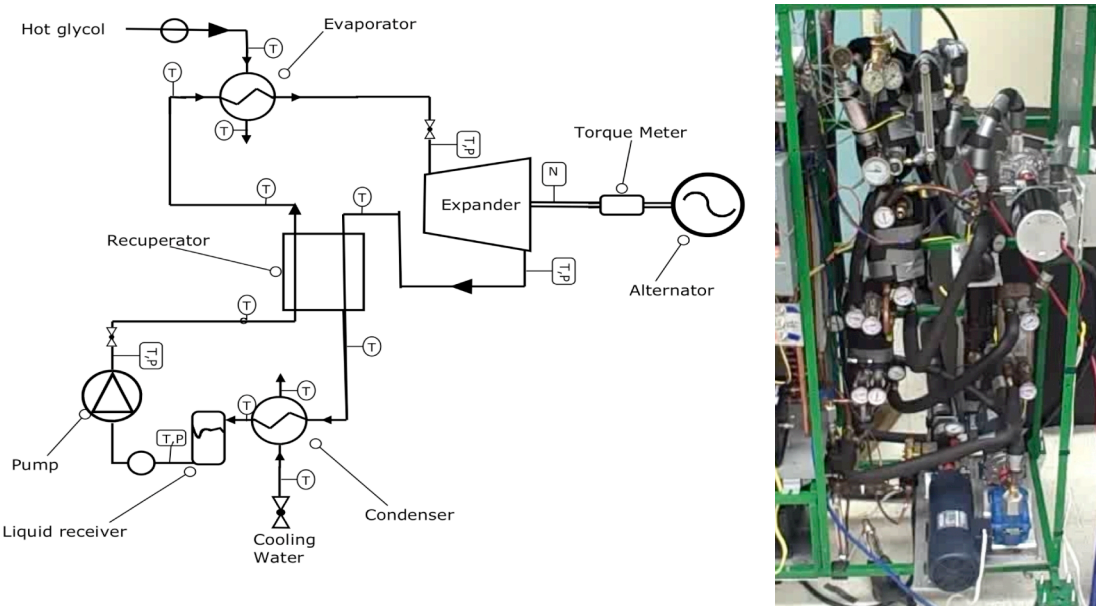

Figure 6: Schematic (above) and photo (right) of the MIT ORC test rig. The rig utilizes Type T thermocouples, pressure transducers, and 0.1% accurate turbine flow meters to establish the intercomponent thermodynamic states. Output is measured via a torque/RPM meter (open drive) or a power analyzing load bank (hermetic).

The expander is arguably the most critical ORC component influencing overall cycle efficiency, followed by the working fluid pump [13]. While traditional turbomachinery is costly at small scales, many positive displacement machines can be adapted from e.g. automotive and HVAC compressor duties to perform as expanders for this application [2-3]. A well-instrumented test ORC was developed (**Fig. 6**) to experimentally measure information required to establish thermodynamic states at discrete points around the closed cycle; this data can be used to calculate the energy balance across any individual component. A range of operating conditions can be imposed to generate performance maps for the expander isentropic efficiency with respect to controlling factors such as pressure ratio, RPM, leakage and friction, and mass flow (throttling) [14, 15]. Testing at MIT and the University of Liege has mapped the performance of several commonly available automotive and HVAC positive displacement scroll machines as ORC expanders using R-245fa or R123 as the working fluid. The various tradeoffs among working fluids described in the literature [16-19], including thermal properties, freezing, sub-ambient condensing pressures, "dry" vs. "wet" expansion, cost and environmental considerations, led to the choice of fluids used. Both fluids demonstrate acceptable performance, including operating pressure ratios low enough to accommodate scroll expander built-in volume ratios, which typically range from 2-5. Using the ORC test bench, measured expander isentropic efficiencies up to 76% (**Fig. 7**) and expander-generator efficiencies up to 64% (**Fig. 8**) were observed with

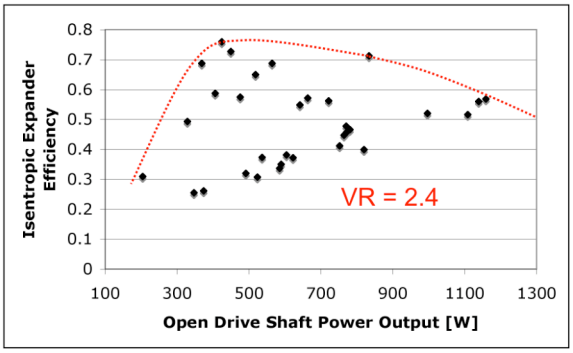

Figure 7: Denso SCSA6 automotive scroll in expander benchmarking. Note: high performance relates to the envelope of multivariate data points projected on a single axis (RPM, leakage, frictional loss, and degree of throttling vary among points).

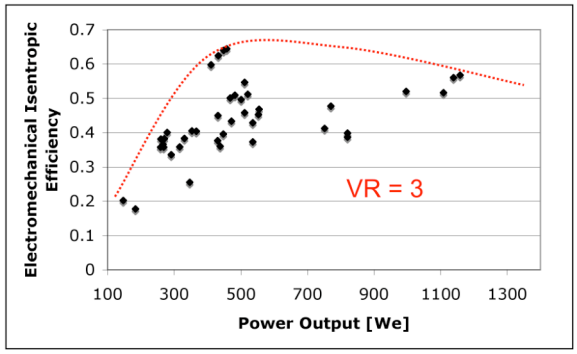

Figure 8: Copeland ZP51K5e commercial HVAC scroll in expander benchmarking. Note: Isentropic efficiency here is the combined efficiency of the coupled expander-generator unit.

built-in volume ratios ranging from 2.4 to 3, resulting in calculated semi-empirical cycle efficiencies of up to 10% for a 150°C solar thermal source (Second Law efficiencies of up to 33%). These results are developed with a combination of performance benchmarking (including measured expander, pump and generator efficiencies) and model predictions using an ORC model in EES developed at the University of Liege (**Fig 9**). For further discussion of the mathematical treatment of the organic Rankine cycle see [13-16]. The bench test results validate the proposed 3 kW solar ORC design currently being implemented in Lesotho southern Africa.

In general, it appears as though mass-produced scroll compressors can be successfully operated as expanders in an ORC with few modifications. Typically it is necessary to remove one or more check valves and defeat any features (relief valves, high temperature protection) that might interfere with reverse operation or high temperature expander duty. In adapting compressors to expander duty, problems may be encountered with premature tip seal wear or galling in scrolls with mating scroll tips, with shaft seal friction and fatigue on open driveshaft scrolls, and with floating seal efficacy in hermetic type HVAC scrolls. These issues vary from make and model and must be overcome on a case-by-case basis.

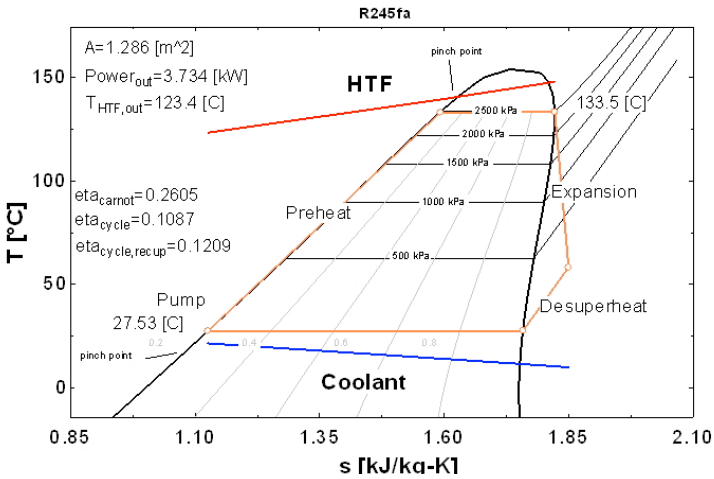

Figure 9: Temperature-Entropy diagram of ORC using R245fa, 1.3m^2 plate heat exchanger area, recuperator and 10°C heat exchanger pinch.

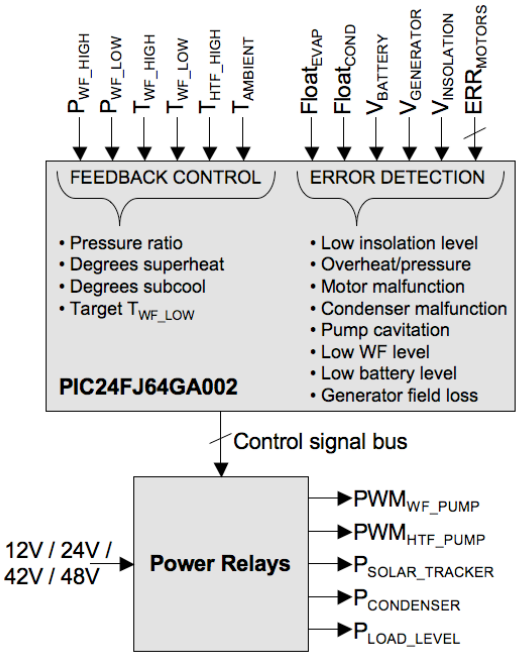

Figure 10: Microcontroller based ORC control.

5. Control

Optimized control of the ORC involves a balance between fixed characteristics of the expander (i.e. optimal pressure ratio, torque vs. RPM characteristics) and the variable heat input delivered from the solar field. This is achieved through a combined analog/digital control architecture that maintains operating parameters within optimal zones via feedback based on input sensor levels.

Control hardware is based on Microchip's PIC24FJ64GA002 microcontroller (3.3V supply, 4 MIPS, 5 16-bit timers, 5 PWM outputs, 21 programmable I/O pins,10 analog inputs with 10-bit conversion and programmable reference voltage, max power draw < 1W) which is programmed via a combination of ANSI C and native assembly code. Semiconductor relays are used to control DC motor speeds via pulse-width modulation (PWM). Type T (*copper-constantan*) thermocouples and Honeywell SPT pressure transducers (stainless steel, temperature compensated, 1% accuracy, 4-20mA output) are used to measure temperature and pressure. Photodiodes (400-800nm) return a proxy for solar insolation level, and Hall effect float sensors (stainless steel case, PTFE float) are used for low fluid level detection to prevent pump cavitation or heat delivery to an evaporator that contains no fluid.

Microcontroller inputs include primary sensor signals, for feedback control, and secondary system measurements, for error condition detection (**Fig. 10**). Primary sensors are sampled at 1-minute intervals, while secondary signals cause a system interrupt under error conditions. Pressure ratio (based on P_{WF_HIGH}, P_{WF_LOW}) and target low-side temperature (based on $T_{AMBIENT}$) are directly calculated from sensor input values. Saturation temperatures are determined for P_{WF_HIGH} and P_{WF_LOW} via a stored T_{SAT} table using linear interpolation between points sampled at 0.5-1 psi. Comparison of these values with T_{WF_HIGH}, T_{WF_LOW} provides the current degree of superheat (for T_{WF_HIGH}) and subcool (T_{WF_LOW}) for the system.

Power signals for the WF (PWM_{WF_PUMP}) and HTF (PWM_{HTF_PUMP}) pump motors and the condenser fans ($P_{CONDENSER}$) are adjusted based on the sensor inputs and derived values. HTF pump speed is adjusted to deliver fluid at approximately 150°C at the outlet of the solar field; that is, a value of T_{HTF_HIGH}<150°C will result in an increased duty cycle, while T_{HTF_HIGH}>150°C will result in a decreased duty cycle. Similarly, the amount of cooling provided by the condenser fans is adjusted such that T_{WF_LOW} is near the optimal value (calculated above from $T_{AMBIENT}$), has between 2-10°C of subcool, and consumes only as much power as is required to achieve these two conditions. Finally, WF pump speed is adjusted to optimize pressure ratio and degree of superheat at the expander inlet (<5°C); note that this adjustment is co-optimized with the allowed load level (P_{LOAD_LEVEL}) on the expander-generator.

Some error conditions create transient changes to power signals (pump cavitation, generator field loss, low insolation level, low WF level in the evaporator) from which the system can recover and continue operation while others trigger a full system shutdown (overheat, overpressure, motor or condenser malfunction, low battery level) after which a manual user reset is required. Note, however, that persistent detection of error conditions from which the system can typically recover may indicate that system maintenance is necessary and a full system shutdown will occur in these cases.

6. Conclusion

Experimental results indicate that unattended kilowatt scale CSP in the CSP-ORC format is achievable at installed costs of ~\$6 $Watt^{-1}$ (equivalent to large systems like the 1 MW APS Saguaro plant) [20], by virtue of inexpensive solar field and heat engine components and at slightly decreased efficiency (solar to electric ~5%). The larger footprint may not be a significant impediment to deployment in areas currently served by diesel or PV.

The expander is an important component to optimize for effective small-scale solar ORC deployment. No purpose-built commercial expander exists for this application, however, one can be adapted from HVAC compressors. Automotive scrolls, though relatively inexpensive and widely available, generally use driveshaft and tip seals (excepting the Denso ES18) that are vulnerable to wear. They are also only available in limited displacements (typically <200cc rev^{-1}) and output less than 1 kilowatt. Hermetic HVAC scrolls have the drawback that internal access entails opening the steel shell and welding flanges to the body and top cap, as well as the need for mechanical reinforcement (e.g. with springs) of the OEM floating seal mechanism for expander operation. In our experience however, the latter type of mass-produced scroll is ideal for small scale solar ORC duty due to (1) inherent axial and radial compliance, (2) a wide assortment of available displacements from a variety of manufacturers (Copeland, Danfoss, etc.), and (3) the built-in single or three phase induction motor which can be operated as a an efficient (>70% mechanical to electrical) generator when synchronized with an AC source or in stand alone mode with appropriately sized run capacitors for maintaining field inductance [21].

Finally, optimized control of the ORC is necessary to obtain the balance between fixed characteristics of the fluid machinery and the variable input from the solar field. This can be achieved through a feedback control architecture that maintains operating parameters within optimal zones by adjusting working fluid flow and heat transfer rates. Dynamic effects (e.g. feedpump cavitation from rapid shift in coolant flow or temperature) are addressed via sensor feedback and restorative operational modes. Autonomous control systems enable unattended operation in remote locations. To test this assertion field trials of a 3 kWe, 70 m^2 parabolic trough solar ORC technology are underway at a rural health clinic in Lesotho, southern Africa.

7. Acknowledgements:

World Bank DM'06, EPA P3, National Collegiate Inventors and Innovators Alliance, MIT Energy Initiative

8. References

[1] García-Rodrígueza and Blanco-Gálvez, Solar-heated Rankine cycles for water and electricity production: POWERSOL project, Desalination 212 (2007), Excellent Press, London.

[2] Kane, et. al., Small hybrid solar power system, Energy 28 (2003) 1427-1443

[3] Singh, R. and Srinivasan, J. "Modified refrigerant compressor as a reciprocating engine for solar thermal power generation" International Journal of Energy Research, Vol. 12, 69-74 (1988)

[3] Barber, Robert, "Current Costs of Solar Powered Organic Rankine Engines" Solar Energy Vol. 20 pp 1-6

[4] Kiceniuk, T. "Development of an Organic Rankine-Cycle Power Module for a Small Community Solar Thermal Power Experiment" DOE/JPL-1060-80 January 15, 1985

[5] Monahan, J. and McKenna, R., 1976, "Development of a 1-kW Organic Rankine Cycle Power for Remote Applications," Proceedings of 1976 IECEC, No. 769199

[6] Nguyen, Khanh Q. "Alternatives to grid extension for rural electrification: Decentralized renewable energy technologies in Vietnam" Energy Policy 35 (2007) 2579-2589

[7] Banerjee, Rangan, "Comparison of options for distributed generation in India" Energy Policy 34 (2006) 101-111

[8] Roth, Ian F, Ambs, Lawrence L. "Incorporating externalities into a full cost approach to electric power generation life-cycle costing" Energy 29 (2004) 2125-214

[9] Price, et. al. "Advances in Parabolic Trough Solar Power Technology" ASME Journal of Solar Energy Engineering, Vol. 124 pp. 109-125 May 2002

[10] Forristall, R. "Heat Transfer Analysis and Modeling of a Parabolic Trough Solar Receiver Implemented in Engineering Equation Solver" NREL/TP-550-34169 October 2003

[11] SCHOTT memorandum on solar thermal power plant technology, Mainz 2005, download: http://www.schott.com/solar/

[12] Gordon, J.M. and Huleihil, Mahmoud, "General performance characteristics of real heat engines," J. Appl. Phys. 72 (3), August 1992

[13] Gu, W. et al. "Theoretical and experimental investigation of an organic Rankine cycle for a waste heat recovery system" Proc. IMechE Vol. 223 Part A: J. Power and Energy

[14] Lemort V., Quoilin S., and Lebrun J., "Numerical simulation of a scroll expander for use in a Rankine Cycle" International Compressor Engineering Conference at Purdue, July 14-17, 2008

[15] S. Quoilin, M. Orosz and V. Lemort "Modeling and experimental investigation of an Organic Rankine cycle using scroll expander for small scale solar applications" EUROSUN 2008 Proceedings

[16] S. Devotta and F.A. Holland "Comparison of theoretical rankine power cycle performance data for 24 working fluids"*Heat Recovery Systems* Vol 5, No 6, pp 503-510, 1985

[17] A. Borsukiewicz-Gozdur and W. Nowak "Comparative analysis of natural and synthetic refrigerants in application to low temperature Clausius–Rankine cycle" Energy 32 (2007) 344–352

[18] Tchanche, B. F., et al. "Fluid selection for a low-temperature organic Rankine cycle" Applied Thermal Engineering 29 (2009) 2468-2476

[19] Zyhowski, Gary J. "HFC-245fa in Organic Rankine Cycle Applications", Honeywell Download: http://www.honeywell.com/sites/portal?smap=gen&page=organicrank&theme=T8

[20] S. Canada et. al. "Status of APS 1-MWe Parabolic Trough Project" NREL/CP-550-39205 Nov. 2005

[21] N. Smith, "Motors as Generators" 2nd ed. Practical Action Publishing, 2008